A Real-Time Battery Thermal Management Strategy for Connected and Automated Hybrid Electric Vehicles (CAHEVs) Based on Iterative Dynamic Programming

Chong Zhu, *Member, IEEE*, Fei Lu, *Member, IEEE*, Hua Zhang, *Member, IEEE*, Jing Sun, *Fellow, IEEE*, and Chunting Chris Mi, *Fellow, IEEE*

***Abstract*—Connected and automated hybrid electric vehicles (CAHEVs) are a potential solution to the future transportation due to their improved fuel economy, reduced emissions, and capability to mitigate congestion and improve safety. The battery thermal management (BTM) in CAHEVs is one of the crucial problems, because the lithium-ion batteries are highly temperature sensitive. Therefore, a practical and energy-efficient BTM strategy is required for both improving the operating temperature of batteries and saving energy. In this study, the dynamic programming (DP) is implemented for a BTM system in CAHEVs for achieving the optimal cooling/heating energy savings for batteries. To enhance the real-time capability, an iterative approach is proposed to approximate the optimum control strategy iteratively in a multi-dimensional search space. The proposed iterative DP strategy can improve the system performance and energy-efficiency by fully exploiting the future road information in CAHEVs combined with a model predictive control method. The hardware-in-the-loop validation of the proposed strategy is conducted on the UDDS and the WLTC drive cycles based on a Toyota Prius PHEV model. The results demonstrate the feasibility and effectiveness of the proposed BTM strategy that leads to a considerable BTM energy reduction.**

***Index Terms*—Battery thermal management (BTM), connected and automated hybrid electric vehicle (CAHEV), energy saving, iterative dynamic programming.**

I. Introduction

HYBRID Electric Vehicles (HEVs) provide better fuel economy and reduced exhaust emission compared with conventional vehicles powered by internal combustion engines [1]. Recently, connected and automated driving has been applied to HEVs to improve fuel economy further as well as the safety [2]. With advanced sensors, the connected and automated HEVs (CAHEVs) can use information of local road and traffic conditions for real-time decision making, thereby leading to a considerable reduction of congestion, travel time, and fuel consumption [3].

One of the key technical challenges in CAHEVs is the battery thermal management (BTM). The commercial Lithium-Ion batteries in HEVs cannot produce enough power under low temperatures because of diminished available energy of cells [4]. Moreover, high working temperatures severely degrade the Lithium-Ion batteries' endurance and may subject the batteries to unsafe that could even result in an explosion. Therefore, the battery packs have to work within 15∼35 °C to improve the state of health (SOH) and ensure safety, sustained power, and long service life [5].

Most automakers adopt active air and liquid combined BTM systems in HEVs due to the tradeoff between performance, durability, and cost [6]. Therefore, researchers have focused on active BTM strategies with external air and liquid cooling/heating flows to improve both the performance and efficiency. [7]–[9] developed the detailed electro-thermal model of the BTM system, which analyzed heat generation, heat dissipation, and temperature distribution. To estimate the internal temperature of the battery, [10], [11] used online observers to identify the battery temperature difference between the surface and the core. For better energy-efficiency, several global optimization methods, such as Pontryagin's maximum principle [12], nonlinear programming [13], and heuristic rules [14], have been performed on predefined road cycles to acquire optimal battery temperatures with lowered BTM energy consumption.

However, the real road and traffic situations cannot be represented by present road cycles because of some stochastic circumstances, e.g., climates and traffic congestion. Consequently, the uncertainties of real drive cycles degrade performance and efficiency of these offline BTM strategies. To deal with this issue, some researchers applied nonlinear model predictive control (NMPC) as real-time capable BTM strategies for HEVs [15], [16]. However, the computational complexity of the NMPC method limits the prediction horizon length; thus the merit of future drive profile prediction in CAHEVs is not fully exploited for energy saving.

Manuscript received February 9, 2018; revised April 27, 2018; accepted May 26, 2018. Date of publication June 6, 2018; date of current version September 17, 2018. The review of this paper was coordinated by Prof. D. Diallo. This work was supported by the U.S. Department of Energy under Grant DE-AR0000797. *(Corresponding author: Chunting Chris Mi.)*

C. Zhu, F. Lu, H. Zhang, and C. Mi are with the Department of Electrical and Computer Engineering, San Diego State University, San Diego, CA 92182 USA (e-mail: chong.zhu@sdsu.edu; feilu@umich.edu; hzhang@mail.sdsu.edu; cmi@sdsu.edu).

J. Sun is with the Department of Naval Architecture and Marine Engineering, University of Michigan, Ann Arbor, MI 48109 USA (e-mail: jingsun@umich.edu).

Color versions of one or more of the figures in this paper are available online at http://ieeexplore.ieee.org.

Digital Object Identifier 10.1109/TVT.2018.2844368

In recent studies [17], [18], the dynamic programming (DP) method has shown its excellence in finding the best global optimal input and state trajectories, especially with nonlinear models. At each time step, DP calculates every possible combination of control inputs and states, e.g., battery temperature, air flow mass rate, and liquid flow mass rate. Thus, DP method can ensure the optimum control of the battery temperature with the minimum energy consumption. In performing DP, continuous control signals and states are quantized for cost-to-go calculation and evaluation at each point of the time, leading to so-called "curse of dimensionality" and demanding a high computational ability. Moreover, the required memory size of the processor is massive if fine grids are used for the control signal and state grids to achieve accurate solutions. The high demands of computational capability and memory size limits the real-time implementation of DP method on the BTM system. Thus, DP has been used primarily for offline optimization. Meanwhile, DP methods with reduced computation such as iterative DP [19], analytical DP [20], and neural-network-based DP [21] were developed for real-time implementations.

In this study, we develop a real-time BTM strategy for CAHEVs to adapt the real road and traffic conditions during driving; thereby the future drive profile prediction can be fully utilized to optimize the air and liquid mass flow for the BTM system. To take advantage of the global optimization capability of DP method in real-time applications, an iterative approach is proposed to reduce the computational demand and memory requirements for the electronic control units (ECUs) in CAHEVs. With the enhanced real-time capability, a long-prediction horizon (up to 30 steps) for the battery temperature can be implemented by the developed thermo-electric model. Thus, a better evaluation of BTM system inputs can be achieved. Moreover, due to the reduced computational efforts by the proposed iterative approach, the optimal BTM control inputs can be achieved within a very short control period, e.g., only 1 second, ensuring the optimal control trajectory can be updated at each sampling and control period. As a consequence, the proposed real-time BTM strategy leads to a better temperature regulation performance and a considerable reduction in cooling/heating energy compared to those using traditional PID-based methods.

Based on a 2010 Toyota Prius PHEV model, the proposed method is validated on the hardware-in-the-loop (HIL) test bench. The parameter sensitivity of the proposed method is also analyzed via the HIL tests. With the significantly improved real-time capability, the algorithm containing a 30 s prediction horizon and 1 s sampling time can be executed within 1 s by the emulated ECU. The test results also show that the proposed real-time BTM strategy can effectively reduce the cooling/heating energy consumption on the drive cycle, which is desirable for CAHEVs.

II. Configuration and Mathematical Model of BTM System in CAHEVs

A. BTM System Configuration in HEVs

The generally applied active air cooling/heating system usually uses fans to drive the cabin air directly flowing over the surface of the battery pack. Due to its low-cost and reliability, the air-based BTM system is preferred by HEV manufacturers [5]. However, for battery cells discharging at high C-rates in plug-in HEVs, the liquid cooling/heating is more suitable due to its higher heat rejection capability, but will increase complexity, cost, and power consumption. To take advantage of both systems, some manufacturers implement air and liquid combined cooling/heating in PHEV models to achieve the optimal performance and efficiency [6]. The architecture of this BTM system is shown in Fig. 1.

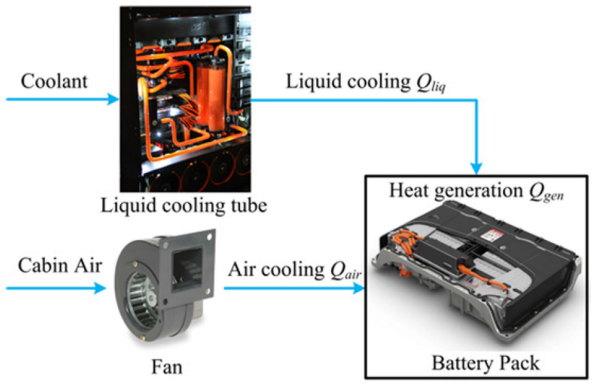

Fig. 1. An Air and indirect liquid combined BTM system for HEVs.

B. Control-Oriented Model

To accurately capture the interplay of the batteries' electrical and thermal behaviors, a control-oriented thermoelectric model is developed for the implementation of model predictive BTM strategy. As shown in Fig. 2(a), the battery electrical behavior is described by an equivalent circuit containing a voltage source V_{oc} and an internal resistance R_{bat} [7]. The battery charge/discharge current can be expressed by

$$I_{bat} = P_{bat}/V_{bat} \tag{1}$$

where P_{bat} is the battery power, and the terminal voltage V_{bat} can be represented as

$$V_{bat} = V_{oc} - R_{bat} I_{bat}. \tag{2}$$

Substituting (1) into (2), the battery charge/discharge current can be calculated as

$$I_{bat} = \left(V_{oc} - \sqrt{V_{oc}^2 - 4P_{bat}R_{bat}}\right)/2R_{bat}. \tag{3}$$

According to (4), the change rate of the battery's state of charge (SOC) can be expressed as

$$\dot{\mathrm{SOC}} = -I_{bat}/C_{bat} = \left(\sqrt{V_{oc}^2 - 4P_{bat}R_{bat}} - V_{oc}\right)/2R_{bat}C_{bat}. \tag{4}$$

In reality, the open-circuit voltage V_{oc} and internal resistance R_{bat} are influenced by the battery temperature and SOC [22], as shown in Fig. 2(b) and (c). Their values can be obtained through offline tests and restored in processors for lookup. In CAHEVs, the future information of battery power P_{bat} can be predicted by the intelligent traffic controllers, providing the possibility to implement predictive thermal management strategy.

As for the controller design purpose, the battery cell is considered as a lumped mass with the same core and surface temper-

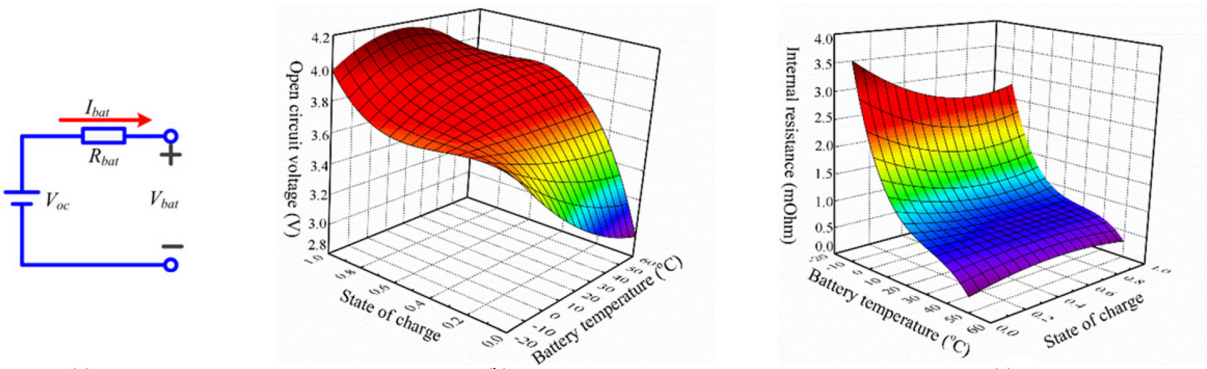

(a) (b) (c)

Fig. 2. The proposed battery electric model. (a) Equivalent circuit diagram of the battery pack. (b) Open-circuit voltage of battery cell. (c) Internal resistance of battery cell.

atures. Thus, a lumped-parameter thermal model is established for its effectiveness in representing the battery temperature dynamics. As shown in Fig. 1, any change in battery temperature can be described as the heat generation and the heat dissipated by the air and liquid flowing around the module:

$$\dot{T_{bat}} = \left(Q_{gen} - Q_{air} - Q_{liq}\right) / C_{p,bat} m_{bat} \tag{5}$$

where Q_{gen} denotes the heat generation rate, Q_{air} and Q_{liq} are rates of the heat dispersed by air and liquid flows, respectively. $C_{p,bat}$ and m_{bat} stand for the module thermal capacity and mass.

The general energy balanced battery thermal model is developed in [6] for estimating the heat generation rate of the battery pack:

$$Q_{gen} = I_{bat}^2 R_{bat} - I_{bat} T_{bat} \frac{dV_{oc}}{dT_{bat}}. \tag{6}$$

The heat generation rate comprises two heat source terms: the *Joule* heat caused by the internal resistance (the first item) and the entropy change (the second item). Usually, the entropy heat generation is only about 5% of total heat generation and can be neglected. Meanwhile, the heat dissipation model can be established using the theory of the uniform wall [23]; thus Q_{air} and Q_{liq} can be calculated by

$$\begin{aligned} Q_{air} &= C_{p,air} m_{air} \left(T_{bat} - T_{cab}\right) \\ &\quad \times \left[1 - \exp\left(-h_{air} A_{air} / C_{p,air} m_{air}\right)\right] \end{aligned} \tag{7}$$

$$\begin{aligned} Q_{liq} &= C_{p,liq} m_{liq} \left(T_{bat} - T_{liq}\right) \\ &\quad \times \left[1 - \exp\left(-h_{liq} A_{liq} / C_{p,liq} m_{liq}\right)\right] \end{aligned} \tag{8}$$

where $C_{p,air}, C_{p,liq}$ represent the thermal capacity of the air and the coolant; T_{cab} and T_{liq} indicate the temperatures of the cabin air and the coolant, respectively. The equivalent heat transfer areas are A_{air} and A_{liq}, and the corresponding heat transfer coefficients are h_{air} and h_{liq}.

The thermoelectric model of a BTM system is described by (3)-(8), in which the air and liquid mass flow rates m_{air} and m_{liq} are considered as system inputs, and the battery temperature and SOC are system states. The system inputs m_{air} and m_{liq} can be regarded as approximately proportional to the consumed electrical power of air and liquid cooling/heating, namely $P_{air} = K_{air} m_{air}$ and $P_{liq} = K_{liq} m_{liq}$.

C. Battery Thermal Management Problem

In CAHEVs, the future traffic information within several minutes can be predicted for battery temperature and energy optimization. To regulate the battery temperature with the minimum consumed energy, the best combination of air and liquid mass flow rates should be found during the drive cycle in real-time. Assuming the future road information within the period t_f can be predicted, the resulting BTM optimization target can be formulated as

$$\begin{aligned} J(t) = \min_{P_{air}(\cdot), P_{liq}(\cdot)} \Bigg\{ & F\left[T_{bat}\left(t + t_f\right)\right] \\ & + \int_t^{t+t_f} g\left[P_{air}(t), P_{liq}(t)\right] \Bigg\} \end{aligned}$$

$$\begin{aligned} \text{s.t.} \ & \left[\dot{T_{bat}}, \dot{SoC}\right]^T \\ & = f\left[T_{bat}(t), P_{air}(t), P_{liq}(t), SoC(t), P_{bat}(t)\right] \\ & P_{air}(t) \in [0, P_{air\_\max}] \\ & P_{liq}(t) \in [0, P_{liq\_\max}] \\ & T_{bat}(t) \in [T_{bat\_\min}, T_{bat\_\max}] \\ & \text{SOC}(t) \in [0.1, 0.9] \end{aligned} \tag{9}$$

where the instantaneous BTM energy consumption is given by $g[P_{air}(t), P_{liq}(t)] = \beta[P_{air}(t) + P_{liq}(t)]$. β is the weighting coefficient defining the tradeoff between battery temperature control and the energy consumption. Due to the real-time constraints, the nonlinear state equation $f[T_{bat}(t), P_{air}(t), P_{liq}(t), SOC(t), P_{bat}(t)]$ derived from (3)-(8) predict the behavior of the BTM system in the prediction horizon t_f.

The critical high or low temperatures can accelerate the aging of the battery cells, resulting in premature of the battery packs. Thus, the critical high or low temperatures should be both punished by the cost function. As shown in Fig. 3, [15], [16] proposed a temperature punishment function to penalize the critical high or low temperatures, which is implemented in

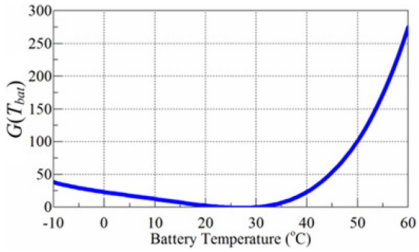

Fig. 3. Battery temperature punishment function.

this study:

$$F\left(T_{bat}\right)=\left(1-\beta\right)\left(\alpha_0+\alpha_1 T_{bat}+\alpha_2 T_{bat}^2+\alpha_3 T_{bat}^3+\alpha_4 T_{bat}^4\right) \tag{10}$$

where α_0, α_1, α_2, α_3, and α_4 are aging coefficients obtained by the curve fitting. The cost function is to manage the battery temperature in the most energy-efficient way with the available air and liquid cooling powers.

III. Conventional Dynamic Programming Algorithm

The main idea of DP method is to grid the problem in time, states and control signals. Each grid point defines a sub-problem that is solved to minimize the sum of a stage cost and the cost-to-go at the next time step and state. In a BTM system, the stage cost at each grid point is defined as the sum of instantaneous air and liquid cooling/heating power. The cost-to-go represents the necessary cost to reach the end of the problem along the optimal state trajectory, which is defined by the tradeoff value between battery temperature and consumed energy in the BTM system.

In order to solve the BTM problem with a DP algorithm, the problem should first be equally discretized into n time steps within the prediction horizon tf. Meanwhile, the battery temperature and SOC can be divided into m discrete points, producing the state vector $x_{i,j}=[T_{bat\_i},\ SOC_j]$ ($i, j = 1, 2, \ldots, m$ denote the state grid index). Thus, a grid of size $n \times m \times m$ over time and state is formed. The DP problem is solved recursively backward in time until reaching the first step, and the cost-to-go values are calculated for all grid points.

The cost-to-go $\boldsymbol{J} \in \mathrm{R}^{n\times m}$ is defined as

$$J_{k-1}\left[i,j\right]=\min_{u_k\in\{P_{air},P_{liq}\}}\left\{\underbrace{g\left(p_{air},p_{liq}\right)}_{\text{stage cost}}+\underbrace{J_k\left[x_{i,j}+f\left(x_{i,j},u_k\right)\right]}_{\text{cost-to-go}}\right\} \tag{11}$$

where $k = n, n-1, \ldots, 2$ denotes time step, and $u_k = [P_{air\_k},\ P_{liq\_k}]$ represents the control signal vector. The cost-to-go at time step n is initialized by the punishment function (10) at each of the discrete state points, e.g., $J_n[j] = F(T_{bat\_j})$. Because the analytical solution of the cost-to-go is unavailable, it is typically evaluated by every possible combination of P_{air} and P_{liq}. Hence, the continuous control signals P_{air} and P_{liq} have to be quantized into a $v \times v$ control grid and interpolate in the cost-to-go. The optimal air and liquid cooling/heating powers are found by minimizing over the quantized control grid. The flow chart of the basic DP method is shown in Fig. 4.

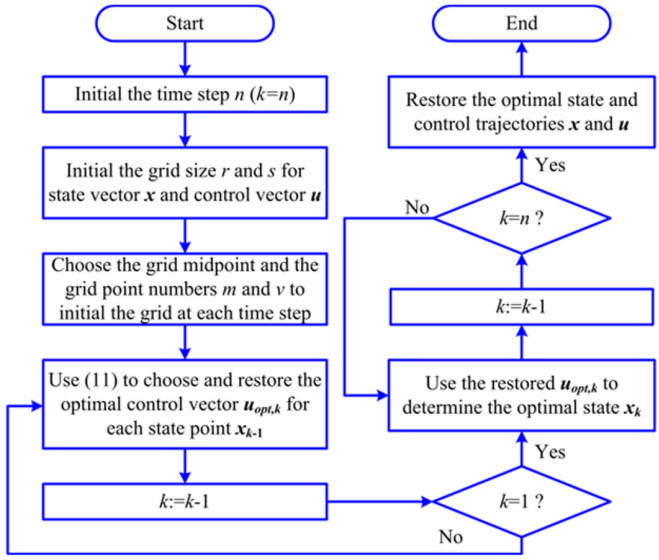

Fig. 4. Flowchart of the basic DP method.

The merit of the DP method is that the global optimum can always be found for discrete control problems. However, the computational demand of the basic DP is high because every control and state grid point should be evaluated to obtain the minimum cost-to-go. Besides, it requires massive processor memory to store the cost-to-go values for interpolation. For instance, when dividing the states T_{bat} and SOC into $(m-1)$ intervals, the memory size should be m^2 to save the state space. The cost-to-go function J is calculated and evaluated for each sub-problem in the control signal grid with $(v-1)$ intervals. Therefore, to find the optimal trajectory of the BTM system, m^2v^2n calculations of the cost-to-go are necessary, as well as m^2n registers to store the cost-to-go values at each time step. In practice, both the state and control signal grid intervals should be refined to reduce numerical errors caused by interpolations, that is, m and v should be large enough to yield the optimal trajectory. Therefore, the "curse of dimensionality" limits the applicability of the basic DP in BTM.

IV. Proposed Iterative DP Algorithm for BTM in CAHEVs

One intuitive method to enhance the applicability of DP is to reduce grid numbers m and v of states and control signals. As the coarse grids result in significant numerical errors, an iterative approach is proposed to reach the optimal trajectories after several repetitive implementations of DP.

A. Iterative Dynamic Programming Algorithm

Iterative dynamic programming (IDP) is a numerical method which reduces the number of sub-problems and computational time by applying the basic DP several times. In the first iteration, the initial optimal trajectory is searched with a coarse control and state grid. Then, the obtained trajectory is chosen as the center point of the grids for re-grid at the next iteration, as

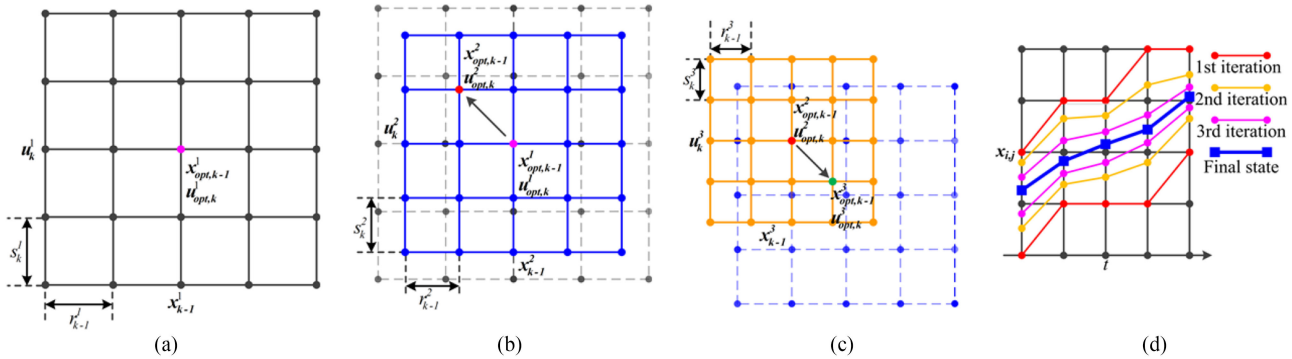

Fig. 5. Reduced grid size and approximate optimal point in IDP. (a) The initial grid. (b) The grid after the first iteration. (c) The grid after the second iteration. (d) Converged upper and lower boundaries during iterations.

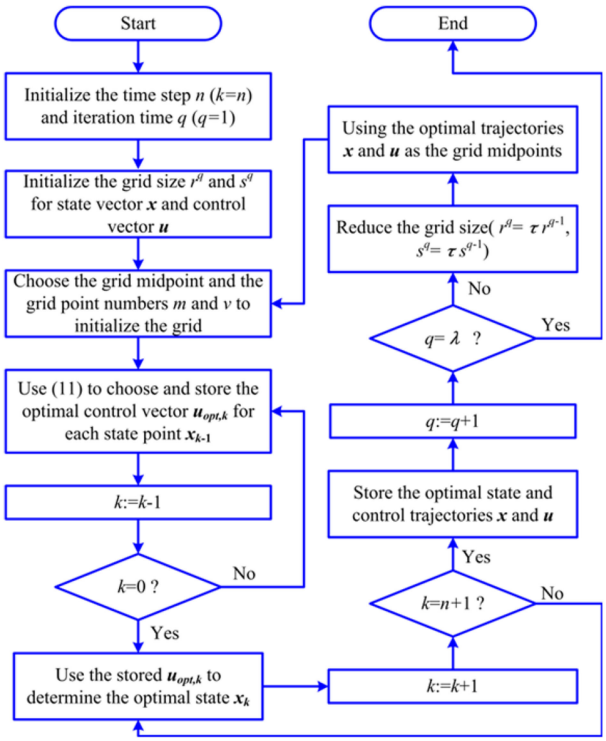

Fig. 6. Flowchart of the proposed iterative DP method.

shown in Fig. 5. The grid size is reduced as the intervals shrink in every iteration, leading to a reduced search range for the optimal trajectory without massive grid points.

The procedure of the IDP algorithm is shown in Fig. 6. At the initial iteration, the basic DP method is implemented to find the optimal control vector $\boldsymbol{u}_{opt,k}$ for each state point $\boldsymbol{x}_{k-1}$ in the grid. Then, the initial optimal state trajectory $\boldsymbol{x}$ and the associated control trajectory $\boldsymbol{u}$ can be determined by substituting $\boldsymbol{u}_{opt}$ into (3)−(8). The obtained state and control trajectories are chosen as the gird midpoints for the next iteration. Once the state grid point number m is fixed, the grid size r is determined by the upper and lower boundaries of the state variables. As the grid sizes r and s are decreased by the reduction factor τ, the search range of the optimal trajectory is reduced for the next implementation of DP algorithm. Therefore, the obtained state and control trajectories can gradually approach the optimum by the iterative executions of DP method until reaching an adequate range of accuracy.

B. IDP Implemented in BTM

The real-time BTM in CAHEVs can be considered as an optimization problem within the prediction horizon t_f. The states are battery temperature and SOC, and the control signals are air and liquid cooling/heating power. The moving horizon in the BTM is divided into $n-1$ discrete time stages, leading to $n-1$ sub-problems. With a predicted battery charge/discharge power, the IDP is used to search for the optimal temperature trajectories and associated control inputs.

The initial control grid at each time step can be determined by $(v-1)$ equally divided space intervals of $P_{air\_\max}$ and $P_{liq\_\max}$, while the initial state grids of battery temperature and SOC should be carefully chosen. A wide range of state variables increases the grid size r, where more iteration times are required to reduce the numerical errors of the optimum trajectory. Contrarily, the optimum trajectory may lie out of the state grid boundary if the initial grid size r is too small. In the BTM system, the predicted battery charge/discharge power P_{bat} can be utilized to determine the upper and lower boundaries of the battery temperature. For example, during battery cooling, the minimum possible battery temperature during each time interval is obtained by using the full power of both air- and liquid-based systems.

The weighting coefficient β in the cost-to-go function (11) affects the performance of the proposed IDP-based BTM strategy. When β is close to 1, the cost-to-go function intends to select the control inputs that can save more energy, but the performance of the battery temperature regulation is degraded at the same time. Contrarily, the battery temperature is better regulated at the expense of decreased efficiency if β is chosen close to 0.

Following steps 1∼4 in the IDP procedure, the cost-to-go value at each state point at the final time step can be determined and restored for calculating the cost-to-go at the next time step by (11). However, for reducing the computational time and memory size, the grid size is large due to the reduced state point number. Hence, in step 5, the derived state point $[x_{i,j} + f(x_{i,j}, u_k)]$ in (11) is likely to locate between the two grid points at the next time interval, whose cost-to-go value is not calculated and restored in advance. To solve this issue, a

local linear approximation approach is proposed:

$$\tilde{J}_k\left[x_{i,j}+f\left(x_{i,j},u_k\right)\right]=J_k\left[x_{i,j}\right]+\left.\frac{\partial J_k\left[x_{i,j}\right]}{\partial x}\right|_{x_{i,j}}\cdot f\left(x_{i,j},u_k\right)$$
$$=J_k\left[x_{i,j}\right]+\frac{J_k\left[x_{i+1,j}\right]-J_k\left[x_{i,j}\right]}{r_k}f_i\left(x_{i,j},u_k\right)$$
$$+\frac{J_k\left[x_{i,j+1}\right]-J_k\left[x_{i,j}\right]}{r_k}f_j\left(x_{i,j},u_k\right). \quad (12)$$

In (12), a 2-dimension forward difference is utilized to define the partial derivative of the state; then the cost-to-go of the state located between the grid points can be interpolated for searching the best control vector.

After the initial optimal trajectory is found, the points of the obtained trajectory are set to the middle of the two boundaries for the next iteration. Assuming the number of iterations is q, the upper and lower boundaries around the optimal trajectory are depicted by:

$$x_{u,k}^{q+1}=x_{opt,k}^{q}+0.5\tau\left(x_{u,k}^{q}-x_{l,k}^{q}\right) \quad (13)$$

$$x_{l,k}^{q+1}=x_{opt,k}^{q}-0.5\tau\left(x_{u,k}^{q}-x_{l,k}^{q}\right). \quad (14)$$

Similar to the state grid size, the control grid size is also reduced by multiplying λ. As shown in Fig. 6, the DP procedures are repeated within the gradually reduced state and control grids until the optimum trajectories are obtained to minimize the BTM energy consumption.

V. Hardware-in-the-Loop Validation Results

A. HIL Test Configuration

A rapid-control-prototyping (RCP) and HIL combined test bench is developed for the BTM system. The BTM strategy is implemented by the dSPACE MicroAutoBox, which is utilized for emulating the electronic control unit (ECU) in CAHEVs. The dSPACE SCALEXIO hardware is used to emulate the physical model of the BTM system. The urban dynamometer driving schedule (UDDS) and the worldwide harmonized light vehicles test procedure (WLTP) are implemented as the test cycles, and the Toyota Prius 2010 PHEV model is selected as the vehicle model. The related parameters are provided by the technical test report of Idaho National Laboratory [22]. The full powers of the air and liquid cooling/heating systems are 150 W and 700 W, respectively. The temperatures of the cabin air and the coolant are both set to 25 °C. The ambient temperature and the initial battery temperature are both set to 40 °C. From Fig. 3, it is known that the optimal operating temperature for the battery pack is 27 °C. In order to obtain both optimal operating temperature and reduced energy consumption, the weighting coefficient β in (11) is set to 0.5.

B. Computational Burden Reduction by IDP Method

In the HIL test, the prediction horizon is set to 30 s, and the discretized period is set to 1 s. Hence, the number of time step n in the DP problem is 30. Considering the control signals are updated every 1 second, all the calculations have to be finished within 1 s. However, in real applications, the control trajectory is not necessarily updated in every control period, so that the proposed thermal management method can be easily integrated in parallel with the other battery management functions.

TABLE I
Implemented IDP With Different Grid Numbers and Iteration Times

	IDP	DP 1	DP 2 (simulated)
Grid numbers m,v	3	9	29
Iteration times λ	80	1	1
Total calculation times $m^2v^2\lambda n$	194,400	196,830	21,218,430
Total execution time	0.98 s	0.99 s	106.73 s
Required memory size	37.97 KB	3.00 MB	647.52 MB

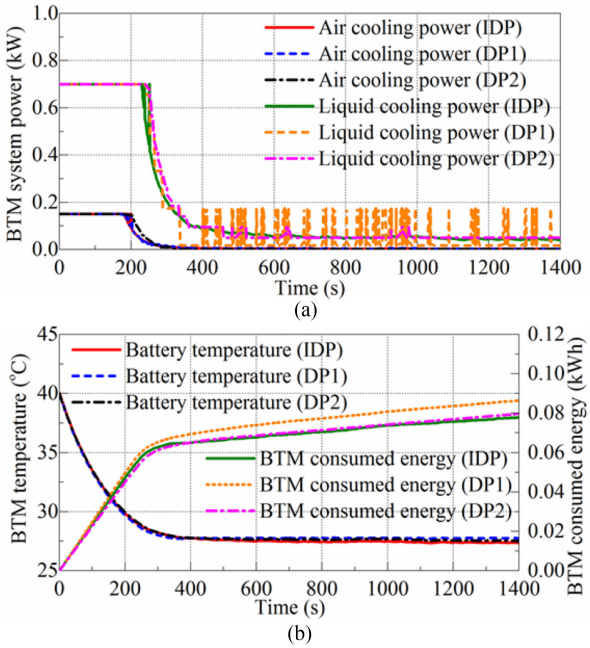

Fig. 7. Comparative HIL test results of IDP method and DP method on UDDS cycle. (a) The air and liquid cooling powers in the BTM system. (b) The battery temperature and the BTM consmued energy.

According to the experiments, the calculation times of the cost-to-go in the MicroAutoBox are limited to less than 200,000 per second. The HIL tests are conducted with the proposed IDP method and the basic DP method without any iteration (DP 1) respectively, as shown in Table I. Due to the limits of the emulated ECU's calculation capability and memory size, the basic DP1 method only has a coarse grid ($m = 9$). In order to provide a comparable performance with the IDP method, the basic DP without iteration is built as DP 2 method with higher grid numbers ($m = 29$), which can be only simulated by the PC.

The test results are shown in Fig. 7. The battery temperature trajectories in Fig. 7(b) are similar for different iterations because the upper and lower boundaries of T_{bat} are well predicted and defined to reduce the grid size. However, The HIL test results indicate that the control trajectories P_{air} and P_{liq} in Fig. 7(a) are much smoother with the proposed IDP method, and the consumed energy for the BTM is also reduced compared with the DP with coarse grids (DP 1). Furthermore, the oscillated control signals by the basic DP method with coarse grids are not applicable for the physical actuators, such as the fan, and the coolant pump in the BTM system. As shown in Fig. 7, if the acceptable performance is required by using the basic DP

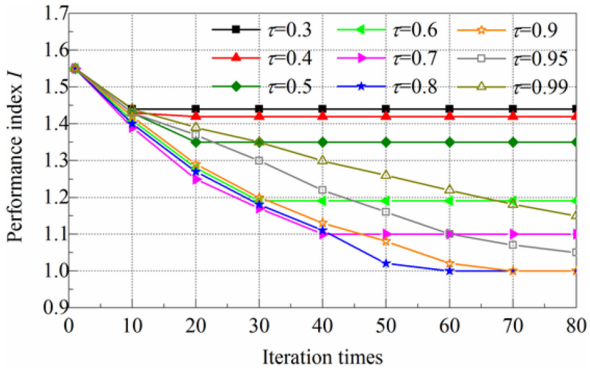

Fig. 8. Performance index over iteration times and grid reduction factor τ.

(DP 2), there is a much higher demand for state and control grid points, leading to significantly increased computational efforts. Moreover, the proposed IDP can considerably reduce the memory size requirement of the processor, as shown in Table I. The results demonstrate that the computational burden and required memory size in the proposed BTM strategy are significantly reduced by the proposed IDP method. The BTM system performance and energy-efficiency are also improved by the IDP method.

The sensitivity of the performance to the grid reduction factor τ is also investigated via the HIL tests where the number of grid points is fixed to 3. The BTM performances is normalized, where $I = 1$ represents the global optimal with the BTM consumed energy being the minimum. As shown in Fig. 8, it is concluded that reduction factor τ lower than 0.7 cannot reach the global optimum even with additional iterations. In those cases, the rapid reduction in the grid size reduces the search range so that the global optimum lies out of the boundaries after a few iterations. However, when τ is close to 1 ($0.9<\tau<1$), it can be seen that the grid converge speed is slow so that the optimal trajectory is not reached within the maximum possible iteration times. Therefore, the optimal grid reduction factor τ is around 0.8 in the BTM system for CAHEVs.

C. Comparative Test Results for System Energy-Efficiency

To verify the energy-efficiency of the proposed IDP-based BTM strategy, a commonly used PID-based BTM strategy in HEVs is also tested for comparison. In this classical method, two PID controllers are used to regulate the air and liquid cooling/heating power, combined with a state-machine to determine whether the liquid cooling/heating should be on or off according to predefined battery temperature levels.

The performances of the tested BTM strategies on UDDS are presented at first. As shown in Fig. 9(b), the battery temperatures' profiles under the two tested methods are very similar, whose dynamics and final states are close to each other. The total BTM consumed energy, namely $W_{air} + W_{liq}$ shown in Fig. 9(b), is almost 20% better for the IDP solution. The energy-efficiency of the BTM has been improved by using IDP without deteriorating the battery temperature regulation. The difference in system energy-efficiency is due to the different combinations of air-based and liquid-based system powers in the two methods, as shown in Fig. 9(a). Similarly, the test results on WLTP cycle also show that the proposed IDP-based strategy can

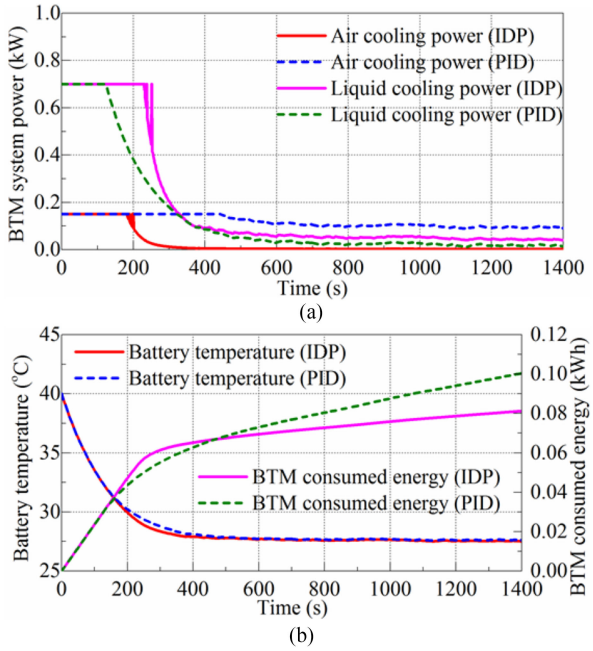

Fig. 9. Comparative HIL test results of classic PID-based and IDP-based BTM strategies on UDDS cycle. (a) The air and liquid cooling powers in the BTM system. (b) The battery temperature and BTM consumed energy.

reduce 14.8% of the BTM energy consumption, representing the good adaptability of the proposed method under various road and traffic conditions.

VI. Conclusion

This study explores the real-time feasibility of optimization algorithms for the battery thermal management in CAHEVs. To improve the system performance and energy-efficiency, a DP-based BTM strategy is proposed to find the global optimum. With the future battery power prediction in CAHEVs, the optimal air and liquid cooling/heating powers are achieved for regulating the battery temperature with the minimum electric energy consumption. An iterative DP method is proposed to mitigate the problems associated with the classical DP to enhance the real-time capability. The HIL validation of the proposed BTM strategy is implemented on a Toyota Prius PHEV model. Compared to the conventional BTM method, the proposed IDP-based BTM strategy can save considerable electric energy for the BTM system on the UDDS and WLTC cycles without deteriorating the battery temperature regulation. The HIL validation results also verify that the real-time capability is significantly improved by the iterative method, making it particularly suitable for CAHEVs.

References

[1] D. W. Gao, C. Mi, and A. Emadi, "Modeling and simulation of electric and hybrid vehicles," *Proc. IEEE*, vol. 95, no. 4, pp. 729–745, Apr. 2007.

[2] D. Bevly *et al.*, "Lane change and merge maneuvers for connected and automated vehicles: a survey," *IEEE Trans. Intell. Veh.*, vol. 1, no. 1, pp. 105–120, Mar. 2016.

[3] S. E. Li *et al.*, "Dynamical modeling and distributed control of connected and automated vehicles: challenges and opportunities," *IEEE Intell. Transp. Syst. Mag.*, vol. 9, no. 3, pp. 46–58, Fall 2017.

[4] J. Jaguemont, L. Boulon, and Y. Dube, "Characterization and modeling of a hybrid-electric-vehicle Llithium-Ion battery pack at low temperatures," *IEEE Trans. Veh. Technol.*, vol. 65, no. 1, pp. 1–14, Jan. 2016.
[5] R. Zhao, S. Zhang, J. Liu, and J. Gu, "A review of thermal performance improving methods of Lithium Ion battery: Electrode modification and thermal management system," *J. Power Sources*, vol. 299, pp. 557–577, Dec. 2015.
[6] G. Xia, L. Cao, and G. Bi, "A review on battery thermal management in electric vehicle application," *J. Power Sources*, vol. 367, pp. 90–105, Nov. 2017.
[7] A. A. Pesaran, "Battery thermal models for hybrid vehicle simulations," *J. Power Sources*, vol. 110, no. 2, pp. 377–382, Aug. 2002.
[8] Y. Hu, S. Yurkovich, Y. Guezennec, and B. J. Yurkovich, "Electro-thermal battery model identification for automotive applications," *J. Power Sources*, vol. 196, pp. 449–457, Feb. 2011.
[9] J. Jaguemont, L. Boulon, P. Venet, Y. Dube, and A. Sari, "Lithium-ion battery aging experiments at subzero temperatures and model development for capacity fade estimation," *IEEE Trans. Veh. Technol.*, vol. 65, no. 6, pp. 4328–4343, Jun. 2016.
[10] R. R. Richardson, and D. A. Howey, "Sensorless battery internal temperature estimation using a Kalman filter with impedance measurement," *IEEE Trans. Sustain. Energy*, vol. 6, no. 4, pp. 1190–1199, Oct. 2015.
[11] Y. Xiao, "Model-based virtual thermal sensors for Lithium-Ion battery in EV applications," *IEEE Trans. Ind. Electron.*, vol. 62, no. 5, pp. 3112–3122, May 2015.
[12] S. Bauer, A. Suchaneck, and F. P. León, "Thermal and energy battery management optimization in electric vehicles using Pontryagin's maximum principle," *J. Power Sources*, vol. 246, pp. 808–818, Jan. 2014.
[13] T. Yuksel, S. Lister, V. Viswanathan, and J. J. Michalek, "Plug-in hybrid electric vehicle $LiFePO_4$ battery life implications of thermal management, driving conditions, and regional climate," *J. Power Sources*, vol. 338, pp. 49–64, Jan. 2017.
[14] D. Feroldi, M. Serra, and J. Riera, "Energy management strategies based on efficiency map for fuel cell hybrid vehicles," *J. Power Sources*, vol. 190, pp. 387–401, May 2009.
[15] J. Lopez-Sanz *et al.*, "Thermal management in plug-in hybrid electric vehicles: a real-time nonlinear model predictive control implementation," *IEEE Trans. Veh. Technol.*, vol. 66, no. 9, pp. 7751–7760, Sep. 2017.
[16] J. Lopez-Sanz *et al.*, "Nonlinear model predictive control for thermal management in plug-in hybrid electric vehicles," *IEEE Trans. Veh. Technol.*, vol. 66, no. 5, pp. 3632–3644, May 2017.
[17] R. Wang and S. Lukic, "Dynamic programming technique in hybrid electric vehicle optimization," in *Proc. IEEE Int. Elect. Veh. Conf.*, 2012, pp. 1–8.
[18] J. Jaguemont, L. Boulon, Y. Dube, and F. Martel, "Thermal management of a hybrid electric vehicle in cold weather," *IEEE Trans. Energy Convers.*, vol. 31, no. 3, pp. 1110–1120, Sep. 2016.
[19] H. G. Wahl and F. Gauterin, "An iterative dynamic programming approach for the global optimal control of hybrid electric vehicles under real-time constraints," in *Proc. IEEE Intell. Veh. Symp.*, Jun. 2013, pp. 592–597.
[20] V. Larsson, L. Johannesson, and B. Egardt, "Analytical solutions to the dynamic programming sub-problem in hybrid vehicle energy management," *IEEE Trans. Veh. Technol.*, vol. 64, no. 4, pp. 1458–1467, Feb. 2015.
[21] Z. Chen, C. C. Mi, J. Xu, X. Gong, and C. You, "Energy management for a power-split Plug-in hybrid electric vehicle based on dynamic programming and neural networks," *IEEE Trans. Veh. Technol.*, vol. 63, no. 4, pp. 1567–1580, May 2014.
[22] "2010 Toyota Prius VIN 0462 Hybrid Electric Vehicle Battery Test Results," Idaho Nat. Lab., Idaho Falls, ID, USA, Rep. INL/EXT-13-28025, Jan. 2013.
[23] M. J. Moran and H. N. Shapiro, *Fundamentals of Engineering Thermodynamics*, 5th ed. New York, NY, USA: Wiley, 2006.

Chong Zhu (M'17) received the B.S. degree in electrical engineering from the China University of Mining and Technology, Xuzhou, China, in 2006 and the Ph.D. degree in electrical engineering from Zhejiang University, Hangzhou, China, in 2016.

He is currently a Postdoctoral Researcher with San Diego State University, San Diego, CA, USA. His research interests include battery thermal management, ac/dc power conversion, and pulse-width modulation techniques applied in EVs.

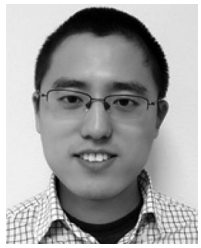

Fei Lu (S'12–M'17) received the B.S. and M.S. degrees from the Harbin Institute of Technology, Harbin, China, in 2010 and 2012, respectively, and the Ph.D. degree from the University of Michigan, Ann Arbor, MI, USA, in 2017, all in electrical engineering.

He is currently a Postdoctoral Researcher with San Diego State University, San Diego, CA, USA. His research topic focuses on the application of electric vehicle charging.

Hua Zhang (S'14–M'17) received B.S., M.S., and Ph.D. degrees in electrical engineering from the Northwestern Polytechnical University, Xi'an, China, in 2011, 2014, and 2017, respectively. From September 2014 to August 2015, she was a joint Ph.D. student funded by the China Scholarship Council with the University of Michigan, Dearborn.

In September 2015, she started to work with San Diego State University. Her research is about the charging technology of electric vehicles.

Jing Sun received the Ph.D. degree from the University of Southern California, Los Angeles, CA, USA, in 1989, and the B.S. and M.S. degrees from the University of Science and Technology of China, Hefei, China, in 1982 and 1984, respectively. From 1989 to 1993, she was an Assistant Professor with the Department of Electrical and Computer Engineering, Wayne State University. She joined Ford Research Laboratory in 1993 where she worked in the Powertrain Control Systems Department. In 2003, she joined the Faculty of the College of Engineering, University of Michigan, where she is currently Michael G. Parsons Professor and the Chair in the Department of Naval Architecture and Marine Engineering, with courtesy appointments as a Professor in the Department of Electrical Engineering and Computer Science and Department of Mechanical Engineering.

Chunting Chris Mi (S'00–A'01–M'01–SM'03–F'12) received the B.S.E.E. and M.S.E.E. degrees in electrical engineering from Northwestern Polytechnical University, Xi'an, China, and the Ph.D. degree in electrical engineering from the University of Toronto, Toronto, ON, Canada, in 1985, 1988, and 2001, respectively.

He is a Professor and the Chair of electrical and computer engineering and the Director with the Department of Energy-funded Graduate Automotive Technology Education Center for Electric Drive Transportation, San Diego State University, San Diego, USA. Prior to joining SDSU, he was with University of Michigan, Dearborn, from 2001 to 2015.